Soc. Netw. Anal. Min. (2016)6:49
DOI 10.1007/s13278-016-0361-x

ORIGINAL ARTICLE

Refining the clustering coefficient for analysis of social and neural network data

Roger Vargas[1] · **Frank Garcea**[2,3] · **Bradford Z. Mahon**[2,3,4] · **Darren A. Narayan**[5,6]

Received: 16 February 2016 / Revised: 27 June 2016 / Accepted: 1 July 2016

Abstract In this paper we show how a deeper analysis of the clustering coefficient in a network can be used to assess functional connections in the human brain. Our metric of edge clustering centrality considers the frequency at which an edge appears across all local subgraphs that are induced by each vertex and its neighbors. This analysis is tied to a problem from structural graph theory in which we seek the largest subgraph that is a Cartesian product of two complete bipartite graphs $K_{1,m}$ and $K_{1,1}$. We investigate this property and compare it to other known edge centrality metrics. Finally, we apply the property of clustering centrality to an analysis of functional MRI data obtained, while healthy participants pantomimed object use or identified objects.

Keywords Edge clustering centrality · Functional MRI data · Tool viewing · Tool pantomiming

Mathematics Subject Classification 05C12 · 90B18

✉ Darren A. Narayan
dansma@rit.edu

[1] Mathematics and Statistics, Williams College, Williamstown, USA

[2] Department of Brain and Cognitive Sciences, University of Rochester, Rochester, USA

[3] Center for Visual Science, University of Rochester, Rochester, USA

[4] Department of Neurosurgery, University of Rochester, Medical Center, Rochester, USA

[5] School of Mathematical Sciences, Rochester Institute of Technology, Rochester, NY, USA

[6] Rochester Center for Brain Imaging, University of Rochester, Rochester, USA

1 Introduction

In a social network, certain individuals are well connected and are more central to the network than others. Various centrality metrics have been investigated including betweenness centrality, closeness centrality, degree centrality, and eigenvalue centrality (Borgatti et al. 2013; Pavlopoulos et al. 2011). All of these metrics are linked to the same goal—finding a vertex (or vertices) that are most central within a network. However, one can also seek the edge (or edges) with the greatest centrality. This idea has been the topic of studies involving edge betweenness centrality (Girvan and Newman 2002; Newman 2010). The edge betweenness centrality of an edge e is the number of shortest paths between two vertices u and v that contain e, divided by the number of shortest paths between two vertices u and v, summed over all pairs of distinct vertices u and v. Another metric for assessing edge centrality is spanning edge centrality where the centrality of an edge is measured by the ratio of spanning trees that contain it. In this paper we introduce a new property, edge clustering centrality, which measures the centrality of edges in a network.

A property that has been ubiquitous in social network literature has been the *clustering coefficient* (Holland and Leinhardt 1971; Watts and Strogatz 1998). For this property we consider the number of existing friendships in each person's network (including themselves) compared to the total number of possible friendships within this local network. Then these quantities are averaged over all friends. This value is known as the clustering coefficient. In a sense, the clustering coefficient measures how closely knit a community network is. A deeper analysis of the clustering coefficient can be conducted so that we can see which pair is most central to the network, that is, how many people know both people in a particular relationship? This has appeared in the

Published online: 14 July 2016

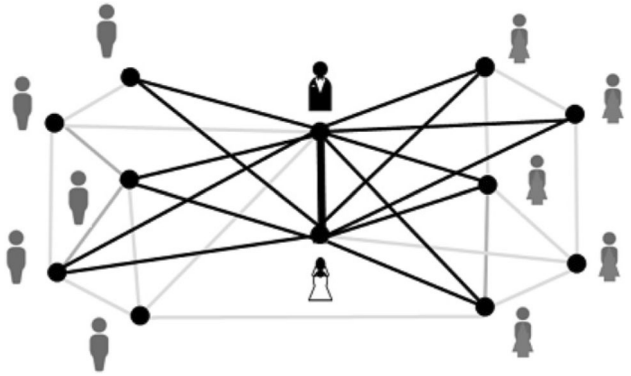

Fig. 1 A wedding network with darker edges showing people connected to both the bride and groom

Fig. 2 A graph with 5 vertices and 8 edges

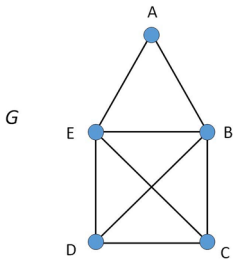

social media, as noted in a *New York Times* article by Alex Williams (www.nytimes.com/2014/08/14/fashion/power-couples-on-twitter-and-instagram.html?_r=0), where celebrity couples have been "leveraging their influence on social media to frame themselves as a public unit, a powerfully synchronous commodity." As part of our analysis, we will investigate the prominence of the influence of a pair in a social network.

A classic example is at a wedding, where guests know either the bride or the groom, and a large number of people know both. In all likelihood, the wedding couple has the most central relationship in the network (see Fig. 1).

We will call this type of analysis "clustering centrality" which is closely related to the clustering coefficient.

Fig. 4 Combination of local subgraphs

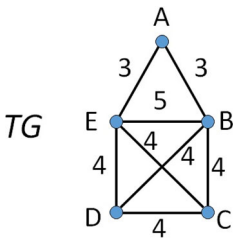

We begin by reviewing the property of the clustering coefficient. The clustering coefficient (closed version) is defined to be

$$\overline{\mathrm{CC}}(G) = \frac{1}{n}\sum_i \frac{2|E(G_i)|}{|V(G_i)| \cdot (|V(G_i)| - 1)}$$

where each local subgraph G_i is the subgraph which includes the vertex i and all of its neighbors. The vertex and edge sets of G_i will be denoted $V(G_i)$ and $E(G_i)$ respectively.

We consider the following example (Fig. 2).

The local subgraphs are as follows (Fig. 3).

For each of the cases, we calculate the number of edges in the local subgraph compared to the number of possible edges: $G_A : 3/3$, $G_B : 8/10$, $G_C : 6/6$, $G_D : 6/6$, and $G_E : 8/10$. The closed clustering coefficient is the average of these fractions: $\overline{\mathrm{CC}}(G) = \frac{1}{5}(1 + 0.8 + 1 + 1 + 0.8) = 0.92$. This high value indicates that the graph is highly connected; however, this single number does not capture some of the finer aspects of this network.

By seeking edges that appear in multiple local subgraphs, we can identify edges that are more important to the network as a whole. We start by combining all of the local subgraphs (counting multiplicities) into a single graph *TG*. The result is shown in Fig. 4.

This idea forms the cases for a new measure which we will call *edge clustering centrality*. The edge clustering centrality of an edge is $C_{\mathrm{cent}}(e) = \sum_i f_i(e)$ where $f_i(e) = 1$ if $e \in E(G_i)$ and $f_i(e) = 0$ if $e \notin E(G_i)$ and G_i is the closed

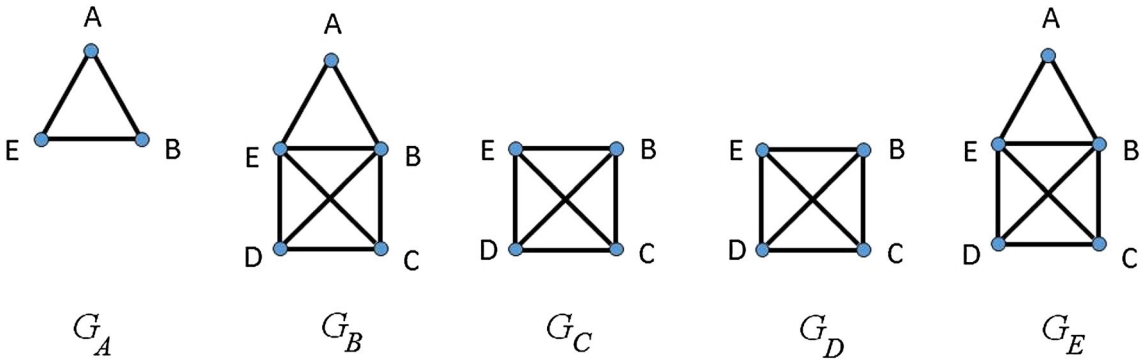

Fig. 3 The local subgraphs of *G*

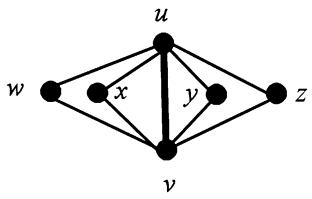

Fig. 5 The book graph B_4 with spine $u - v$

neighborhood of vertex i. In our example, $C_{\text{cent}}(EB) = 5$, $C_{\text{cent}}(BC) = C_{\text{cent}}(BD) = C_{\text{cent}}(CD) = C_{\text{cent}}(CE) = C_{\text{cent}}(DE) = 4$, and $C_{\text{cent}}(AE) = C_{\text{cent}}(AB) = 3$. Since EB has the highest *clustering centrality*, it can be considered more important to the network's connectivity, whereas edges AB and AE can be considered of lesser importance.

In this paper we will explore the property of clustering centrality. We first show it can be formulated as a problem in structural graph theory. Next we show how it differs from other centrality metrics, and finally we apply it to a real-world problem involving the analysis of functional connectivity of the human brain.

2 Edge clustering centrality

Computing the frequencies that edges appear across all local subgraphs is straightforward. The problem of finding the edge with the greatest frequency can be linked to a problem in *extremal* graph theory. The graph shown in Fig. 5 is an example of a Cartesian Product of two complete bipartite graphs $K_{1,m}$ and $K_{1,1}$ and is known as a *book graph* B_m (with $K_{1,1}$ serving as the "spine") (Sun 1994; Liang 1997; Barioli 1998; Shi and Song 2007) and has been a focus of studies in Graph Ramsey Theory (Radziszowski et al. 2014). In our analysis, we will search for the maximum sized book graph H found in a graph G. The spine of the graph H will have the highest edge clustering centrality of any edge in G.

We note that the edge clustering centrality of an edge e in a graph G can be computed simply by counting the number of triangles in G containing e—a computation for which efficient algorithms exist. Looking back to the wedding example in Fig. 1, the darker edges correspond to the book graph B_6.

2.1 Comparison with other edge centrality properties

We next show that edge clustering centrality differs from other known edge centrality metrics, including edge betweenness centrality, κ-path centrality, and spanning edge centrality. The most well-known edge centrality property is *edge betweenness centrality* introduced by Freeman (1977) and later used in modularity algorithms by Girvan and Newman (2002) and Newman (2010).

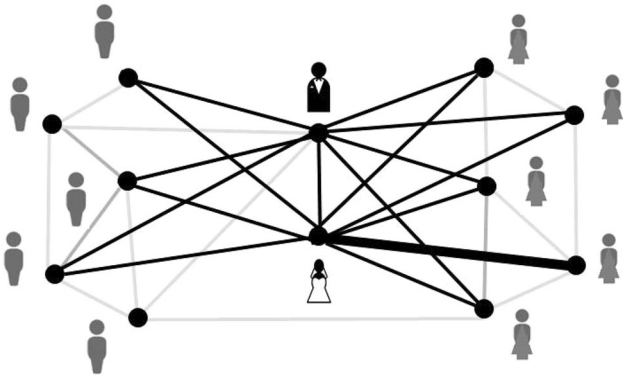

Fig. 6 Betweenness centrality of the wedding network

Definition 1 The edge *betweenness centrality* of an edge e, denoted $bc(e)$, measures the frequency at which e appears on a shortest path between two distinct vertices x and y. Let σ_{xy} be the number of shortest paths between distinct vertices x and y, and let $\sigma_{xy}(e)$ be the number of shortest paths between x and y that contain e. Then $bc(e) = \sum_{x,y} \frac{\sigma_{xy}(e)}{\sigma_{xy}}$ (for all distinct vertices x, and y).

Edge clustering centrality works especially well in dense graphs; however, sparse graphs may have edges that are not contained in any triangles and thus these edges will have an edge clustering centrality of zero. Hence, for sparse graphs such as paths or cycles, edge betweenness centrality would be preferable to use. However, this may not be true for dense graphs. We will show in the next example if the graph contains a book graph as a subgraph, edge clustering centrality can give a better measure of edge centrality.

We consider the graph shown in Fig. 1. Using the betweenness centrality script from MATLAB BGL (https://www.cs.purdue.edu/homes/dgleich/packages/matlab_bgl/), we find that the edge with the largest betweenness centrality is the edge connecting the bride to one of the women on the right (see Fig. 6). As a result while this edge is more central in terms of betweenness centrality, it is may not be the most central edge in the network.

A variant of betweenness centrality is κ-path edge centrality which was proposed by De Meo et al. (2012). Here, the k-path edge centrality index of an edge is the number of shortest paths of length less than or equal to κ that contain the given edge. In graphs with small diameter, κ-path edge centrality will be similar to edge betweenness centrality. Another centrality metric that has appeared in the literature is *spanning edge centrality*, where the spanning edge centrality of an edge is the fraction of the spanning trees that contain the given edge (Mavroforakis

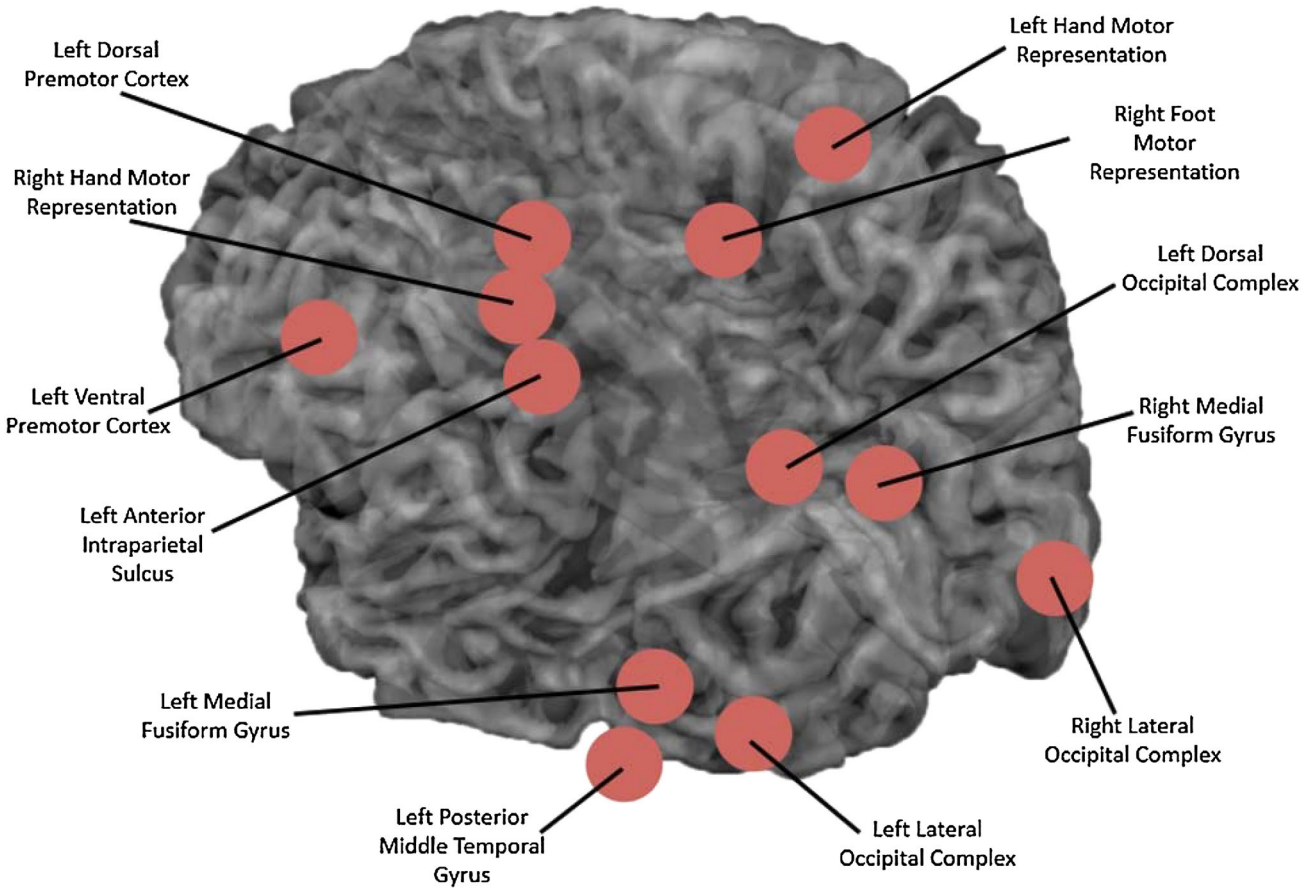

Fig. 7 Brain map with twelve ROIs (reproduced from Fig. 2 in Garcea et al., under review)

et al. 2015). However this metric is only applicable for graphs that are connected. Furthermore, there can be concerns if a graph contains a pendant edge (an edge incident to a vertex with degree one). A pendant edge will typically not be central to the graph, but it will have a high spanning edge centrality (consistent with any cut-edge) since it will appear in every spanning tree.

3 A real-world application

We will use centrality metrics from graph theory to model brain connectivity. In our graph model, the vertices correspond to physical regions of the brain [Regions of Interest (ROIs)], and the undirected edges correspond to a correlation in the functional activation profiles associated with the two vertices. Functional Magnetic Resonance data (fMRI) consist of a time course of Blood Oxygenated Level Dependent (BOLD) contrast (activation) for every voxel in space. Hence, an undirected edge is present in two regions of the brain if there is a strong correlation between the time series of BOLD signals between the respective regions.

In our model of the brain, we have selected 12 regions across the temporal, parietal and frontal lobes (see Fig. 7, reproduced from Fig. 2 in Garcea et al., under review).

Of the 12 regions, the following are considered motor areas: left dorsal premotor cortex, primary motor cortex for the right hand, left ventral premotor cortex, primary motor cortex for the right foot, primary motor cortex for the left hand. Visual areas include the left lateral occipital complex and right lateral occipital complex.

In addition, some of the 12 regions are "tool-preferring", meaning that they exhibit differential BOLD contrast when participants view images of manipulable objects compared to various baseline categories of visual stimuli (e.g., animals, houses). These regions include the left ventral premotor cortex, left dorsal occipital cortex, left and right medial fusiform gyri, the left posterior middle temporal gyrus, and the left inferior parietal lobule (Almeida et al. 2013; Garcea and Mahon 2014). The left and right medial fusiform gyri are associated with visual processing of surface properties of objects, and the Left Dorsal Occipital Cortex is linked to the visual processing of volumetric/3D information about objects. In addition, the Left Inferior Parietal Lobule (Supramarginal Gyrus,

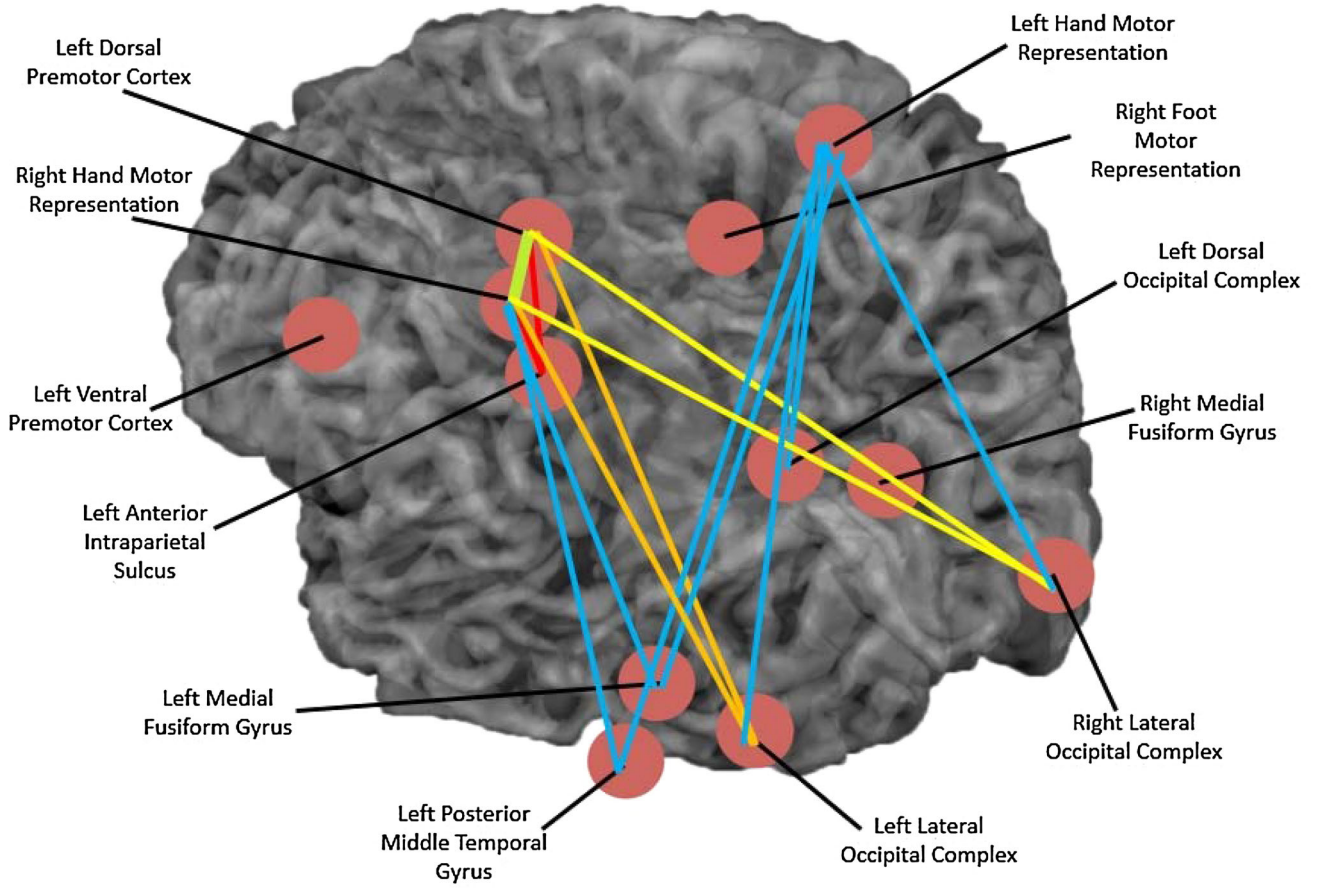

Fig. 8 Edge clustering centrality: pantomiming greater than viewing

Anterior Intraparietal Sulcus) is a region that is important for representing manipulation knowledge (i.e., the knowledge of how to correctly grasp and manipulate an object).

The dataset used in this paper was collected at the Rochester Center for Brain Imaging (University of Rochester) with 12 healthy, right-handed individuals (for full details of the experimental paradigm, MRI acquisition, preprocessing, and analysis, see Garcea et al., under review). Data were collected in two different tasks in which participants were shown images of various tools: hammer, scissors, screwdriver, knife, pliers, and corkscrew. In one task, participants were asked to pantomime the use of a presented object with their right hand during the fMRI, while during the second task participants were asked to and identify the images.

We looked at correlations in BOLD time series between each pair of 12 different regions. A two tailed t test was performed, and statistically significant values (at $t > 2.75$) were selected. For each pair of regions, the temporal correlations in BOLD time series were computed separately for the task in which participants were pantomiming the object use and identifying the objects. The data consisted of two 12×12 correlation matrices for each subjects (one matrix for pantomiming and one for viewing). These matrices were subtracted from one another to create two matrices, one where pantomiming was greater than visual, and a second where the visual was larger than pantomiming.

3.1 Pantomiming greater than viewing

In Fig. 8 we show the edges where pantomiming was greater than for identification. We highlight edges in the largest book graph with red, orange, and yellow representing the different overlapping triangles.

We note in the graph we are seeing stronger connectivity between two of the motor regions: Left Dorsal Premotor Cortex and the Primary Motor Cortex for the Right Hand. We note that Primary Motor Cortex for the Right Foot is not connected to the graph, which is consistent with the fact that the movement of this limb was not prompted by the stimuli.

We note that this network contains the book graph B_3, with a spine between the Left Dorsal Premotor Cortex and the Primary Motor Cortex for the Right Hand, and three other regions: Left Inferior Parietal, Left Lateral Occipital Cortex, and the Right Lateral Occipital Cortex. This is consistent

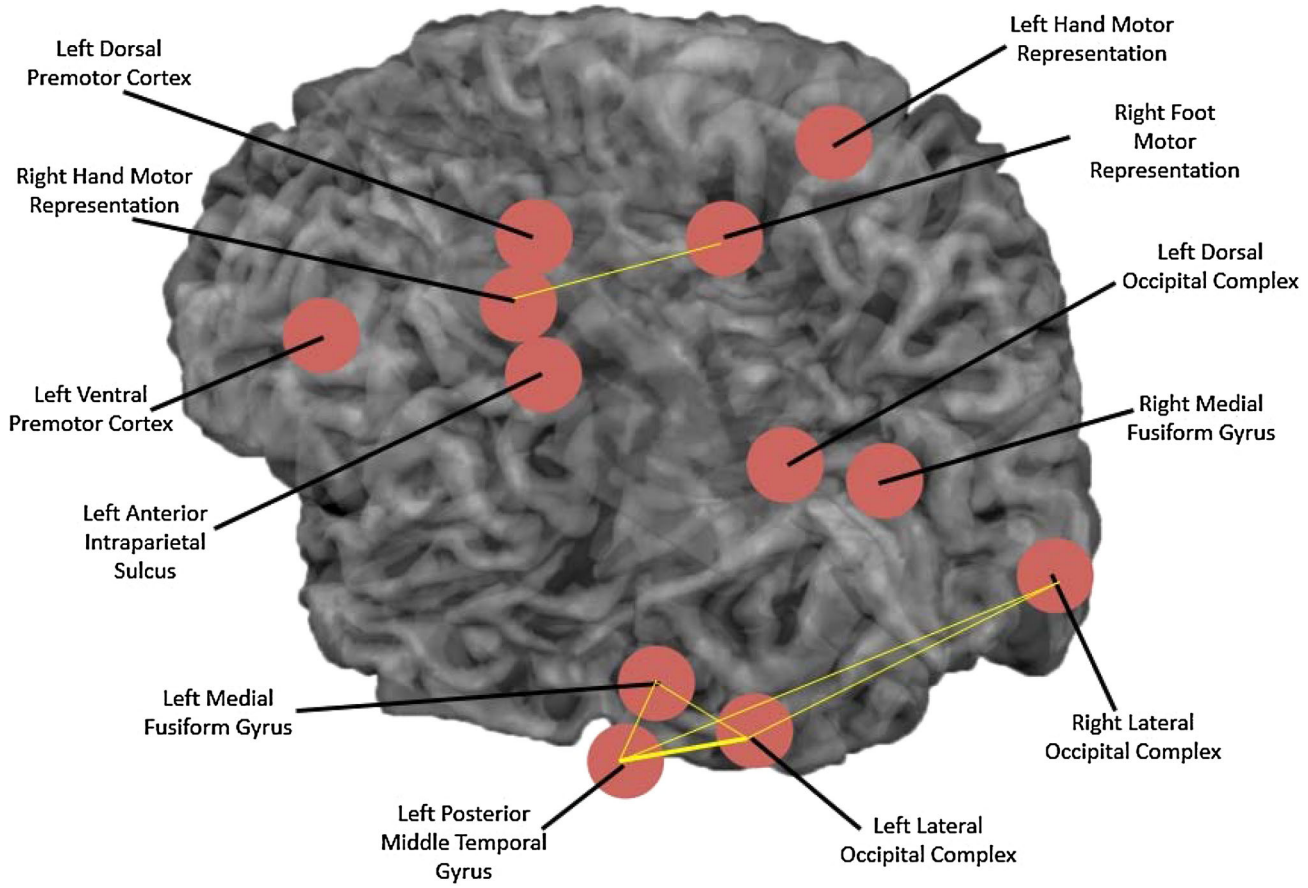

Fig. 9 Edge clustering centrality: viewing greater than pantomiming

with neurological expectations as these three 'are involved in accessing object-directed manipulation knowledge from the visual structure of objects (for details and discussion, see Garcea et al., under review). Furthermore, the result that the Left Dorsal Premotor Cortex is on the spine of the graph is consistent with the fact that both of this motor region is part of the tool network (Garcea and Mahon 2014). Although the Left and Right Lateral Occipital Cortex regions are associated with visual object recognition, there is connectivity between each of them and the motor regions on the book spine. The reason for this is that in order to pantomime a tool, there has to be a connection among visual regions first (as the subject recognizes the tool) and then a connection between motor regions as the tool is manipulated (Almeida et al. 2013; Mahon et al. 2013).

3.2 Viewing greater than pantomiming

In Fig. 9 we show connections where edges are stronger during object identification then during pantomime of object use.

Examining edges that were stronger during visual object identification than pantomiming, we see a network of four regions (Left Medial Fusiform Gyrus, Left Posterior Middle Temporal Gyrus, Left Lateral Occipital Complex, and the Right Lateral Occipital Complex) that form the book graph B_2. These connections are expected since these edges connect regions of the temporal and occipital lobes which support the visual processing and representation of tools. The edge with greatest clustering centrality is the edge between Left Lateral Occipital Complex and Left Posterior Middle Temporal Gyrus and is found in two local subgraphs, and is the "spine" of the book graph B_2.

3.3 Comparison with other edge metrics

As mentioned in the introduction, there are other known methods to quantify edge centrality, including edge betweenness centrality, κ-path edge centrality, and spanning edge centrality.

An analysis using edge betweenness centrality produced results that were similar to those obtained using edge clustering centrality for the network where the pantomiming effects were greater than the viewing effects (see Fig. 10).

We note that κ-path edge centrality will have similar results to edge betweenness centrality as the diameter of the

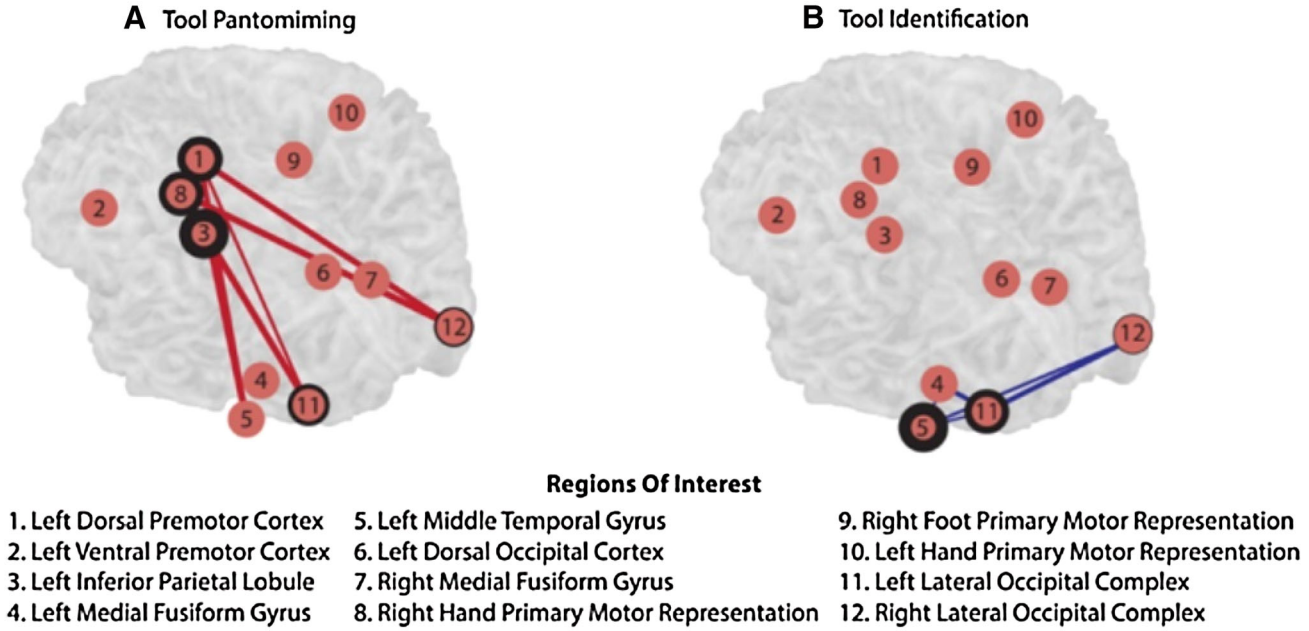

Fig. 10 Stimulus-driven Betweenness Centrality during **a** Tool Pantomiming and **b** Tool Identification Experiments

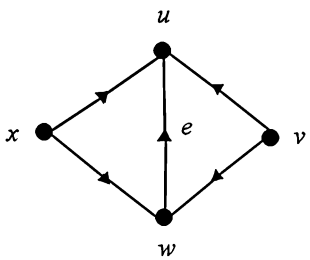

Fig. 11 A directed network

graph is small (4) and there is only one pair of regions (Left Anterior Interparietal Sulcus and the Left Dorsal Occipital Complex) that are distance 4 apart. Spanning edge centrality is not relevant here as the graph is not connected.

4 Conclusion and future work

There are many possible variations for edge clustering centrality which include directed and weighted edges. A directed version could count the number of transitive triangles that contain a given edge. For example, for the graph shown in Fig. 11, the edge *e* is the most central as it is contained in two transitive (acyclic) triangles, while all other edges are only contained in a single triangle.

Another possible variation for directed graphs would be to count the number of directed triangles, or larger cycles that contain a given edge.

Edge clustering centrality could also be modified for use in graphs where the edges have weights. The weighted edge clustering centrality of an edge could then be defined to be the total weight of edges in transitive (acyclic) triangles that contain the given edge.

Acknowledgments Roger Vargas's research was supported by a NSF Research Experiences for Undergraduates Grant at the Rochester Institute of Technology #1358583, under the direction of Darren Narayan. Darren Narayan was also supported by NSF Award #1019532. The acquisition and analysis of the MRI data reported herein was supported by NIH Grant NS089609 to Bradford Mahon. Preparation of this manuscript was supported by NIH Grant NSO89069 and NSF Grant 1349042 to Bradford Mahon. Frank Garcea was supported by a University of Rochester Center for Visual Science pre-doctoral training fellowship (NIH training Grant 5T32EY007125-24).

References

Almeida J, Fintzi AR, Mahon BZ (2013) Tool manipulation knowledge is retrieved by way of the ventral visual object processing pathway. Cortex 49:2334–2344

Barioli F (1998) Completely positive matrices with a book-graph. Linear Algebra Appl 277(1–3):11–31

Borgatti SB, Everett MG, Johnson JC (2013) Analyzing social networks. Sage Publications, Thousand Oaks

De Meo P, Ferrarab E, Fiumaraa G, Ricciardello A (2012) A novel measure of edge centrality in social networks. Knowl-Based Syst 30:136–150

Freeman L (1977) A set of measures of centrality based on betweenness. Sociometry 40:35–41

Garcea FE, Chen Q, Vargas R, Narayan D, Mahon. BZ Task- and domain-specific modulation of functional connectivity in the human brain. Cereb Cortex (Under Review)

Garcea FE, Mahon BZ (2014) Parcellation of left parietal tool representations by functional connectivity. Neuropsychologia 60:131–143

Girvan M, Newman MEJ (2002) Community structure in social and biological networks. Proc Natl Acad Sci USA 99:7821–7826

Holland PW, Leinhardt S (1971) Transitivity in structural models of small groups. Comp Group Stud 2:107–124

Liang Z (1997) The harmoniousness of book graph $St(4k+1) \times P_2$. Southeast Asian Bull Math 21(2):181–184

Mahon BZ, Kumar N, Almeida J (2013) Spatial frequency tuning reveals interactions between the dorsal and ventral visual systems. J Cogn Neurosci 25:862–871

Mavroforakis C, Garcia-Lebron R, Koutis I, Terzi E (2015) Spanning edge centrality: large-scale computation and applications, ACM 978-1-4503-3469-3/15/05. doi:10.1145/2736277.2741125

MatlabBGL. https://www.cs.purdue.edu/homes/dgleich/packages/matlab_bgl/

Newman MEJ (2010) Networks: an introduction. Oxford University Press, Oxford

Pavlopoulos GA, Secrier M, Moschopoulos CN, Soldatos TG, Kossida S, Aerts J, Schneider R, Bagos PG (2011) Using graph theory to analyze biological networks. BioData Min 4:10. doi:10.1186/1756-0381-4-10

Radziszowski S (2014) Small Ramsey numbers, Dynamic Survey #DS1. Electron J Comb

Shi L, Song Z (2007) Upper bounds on the spectral radius of book-free and/or K2, l-free graphs. Linear Algebra Appl 420:526–529

Sun RG (1994) Harmonious and sequential labelings of the book graphs B_m. (Chinese). Gaoxiao Yingyong Shuxue Xuebao Ser A 9(3):335–337

The Power of Two; Power Couples on Twitter and Instagram. www.nytimes.com/2014/08/14/fashion/power-couples-on-twitter-and-instagram.html?_r=0

Watts DJ, Strogatz SH (1998) Collective dynamics of 'small-world' networks. Nature 393(6684):440–442